Allogeneic iPSC-Derived RPE Cell Graft Failure Following Transplantation Into the Subretinal Space in Nonhuman Primates

Trevor J. McGill,[1,2] Jonathan Stoddard,[2] Lauren M. Renner,[2] Ilhem Messaoudi,[3] Kapil Bharti,[4] Shoukhrat Mitalipov,[5] Andreas Lauer,[1] David J. Wilson,[1] and Martha Neuringer[1,2]

[1]Department of Ophthalmology, Casey Eye Institute, Oregon Health & Science University, Portland, Oregon, United States
[2]Department of Neuroscience, Oregon National Primate Research Center, Oregon Health & Science University, Beaverton, Oregon, United States
[3]Department of Molecular Biology and Biochemistry, University of California Irvine, Irvine, California, United States
[4]Unit on Ocular and Stem Cell Translational Research, National Eye Institute/National Institutes of Health, Bethesda, Maryland, United States
[5]Department of Reproductive and Developmental Sciences, Oregon National Primate Research Center, Oregon Health & Science University, Beaverton, Oregon, United States

Correspondence: Trevor J. McGill, Department of Ophthalmology, Casey Eye Institute, Oregon Health & Science University, 3375 SW Terwilliger Boulevard, Portland, OR 97239, USA;
mcgilltr@ohsu.edu.

Submitted: June 19, 2017
Accepted: February 5, 2018

Citation: McGill TJ, Stoddard J, Renner LM, et al. Allogeneic iPSC-derived RPE cell graft failure following transplantation into the subretinal space in nonhuman primates. *Invest Ophthalmol Vis Sci*. 2018;59:1374–1383. https://doi.org/10.1167/iovs.17-22467

Purpose. To characterize the intraocular immune response following transplantation of iPS-derived allogeneic RPE cells into the subretinal space of non–immune-suppressed rhesus macaques.

Methods. GFP-labeled allogeneic iPS-derived RPE cells were transplanted into the subretinal space of one eye ($n = 6$), and into the contralateral eye 1 day to 4 weeks later, using a two-stage transretinal and transscleral approach. Retinas were examined pre- and post-surgery by color fundus photography, fundus autofluorescence, and optical coherence tomography (OCT) imaging. Animals were euthanized between 2 hours and 7 weeks following transplantation. T-cell (CD3), B-cell (CD20), and microglial (Iba1) responses were assessed immunohistochemically.

Results. Cells were delivered into the subretinal space in all eyes without leakage into the vitreous. Transplanted RPE cells were clearly visible at 4 days after surgery but were no longer detectable by 3 weeks. In localized areas within the bleb containing transplanted cells, T- and B-cell infiltrates and microglia were observed in the subretinal space and underlying choroid. A T-cell response predominated at 4 days, but converted to a B-cell response at 3 weeks. By 7 weeks, few infiltrates or microglia remained. Host RPE and choroid were disrupted in the immediate vicinity of the graft, with fibrosis in the subretinal space.

Conclusions. Engraftment of allogeneic RPE cells failed following transplantation into the subretinal space of rhesus macaques, likely due to rejection by the immune system. These data underscore the need for autologous cell sources and/or confirmation of adequate immune suppression to ensure survival of transplanted RPE cells.

Keywords: allogeneic RPE, cell transplantation, graft failure

Age-related macular degeneration (AMD) is the leading cause of blindness in North America and Europe, affecting more than 10 million individuals in the United States alone.[1] Both genetic and environmental factors contribute to its development, although the precise etiology of this condition remains to be elucidated.[2–4] Choroidal neovascularization and geographic atrophy, the advanced forms of AMD, have in common the progressive death of the retinal pigmented epithelium (RPE), associated degeneration of the overlying photoreceptors, and resultant severe central vision loss. Currently no clinical treatments exist for the protection or replacement of vulnerable RPE cells; however, RPE cell transplantation has gained significant interest as a potential therapy. In rodent models of retinal degenerative disease, RPE cell transplantation has been demonstrated repeatedly to be efficacious in minimizing loss of vision and reducing the rate of retinal degeneration.[5–12] As a result, several human clinical trials are under way to evaluate the safety and potential efficacy of RPE cell transplantation.[13,14]

Two primary considerations in developing an appropriate cell-based therapy for AMD patients are the source of the therapeutic cells and the immunological consequences following transplantation. Potential sources of therapeutic cells for use in transplantation studies include pluripotent cells derived from fetal, embryonic, or adult cell sources, which are then subsequently differentiated into RPE cells. Recent research efforts have focused on generation of human induced pluripotent stem cell (iPS) lines from adult cell sources, such as skin (fibroblasts) or blood (peripheral blood mononuclear cells [PBMCs]). Adult sources of cells typically are chosen not only to avoid significant ethical issues surrounding embryonic or fetal stem cells, but also because adult somatic cell sources are plentiful. From an immunological perspective, preclinical

studies in rodent models, regardless of cell source, have generally been performed under xenogeneic conditions (transplantation of human cells into rodents), and thus the long-term survival of the engrafted cells has required protection from immune rejection through the use of immune-suppressive drugs.[7,9,12,15–19] However, for clinical application, therapeutic cells will likely need to be from an allogeneic or an autologous source. Allogeneic cells have decided advantages over autologous cells, as production of one large lot of allogeneic cells could be used to treat many patients, would provide a standardized source, could be administered in a relatively short time-frame, and would be relatively cost-effective. However, administration of allogeneic cells carries significant risk that immune system–mediated rejection will compromise the grafted cells and potentially damage the surrounding tissue, a serious concern in an already diseased retina. If long-term immunosuppressive therapy is required for allogeneic cell therapy, it would raise significant risk/benefit concerns in an elderly population. In contrast, cells derived from autologous (or perhaps even HLA-matched) sources have the significant theoretical advantage of evading detection and rejection by the immune system; however, for each prospective patient, pluripotent and therapeutic cell lines would need to be derived and characterized, requiring a very time-consuming, laborious, and expensive process that may prove prohibitive in practical application. Finally, the cell source can define the immunological conditions under which the cells are transplanted: fetal and embryonic stem cell sources can provide only allogeneic cells for transplantation, whereas iPS-derived cells can be produced for allogeneic or autologous cell transplantation strategies, and thus have a significant advantage over other cell sources.

The field of stem cell–based transplantation as a prospective therapy for retinal disease is relatively young, and few studies have examined the survival and efficacy of allogeneic or autologous cell transplants, either with or without immunosuppression. We demonstrated previously that genetically identical (syngeneic) Schwann cells rescued visual function long-term in the Royal College of Surgeons (RCS) rat model of retinal degeneration, whereas allogeneic cells provided only short-term vision rescue.[20] However, this long-term study was exclusively behavioral in nature, and histological analysis was not performed, so that transplanted cell survival/rejection was not evaluated. More recently, transplantation of iPS-derived allogeneic RPE cells into a non–immune-suppressed pig model demonstrated evidence of immune rejection at 3 weeks posttransplantation.[21] Although an important finding, this study did not characterize the longitudinal adaptive or innate immune responses, which play critical roles in allogeneic responses. Another cell transplantation study explored long-term survival of allogeneic (MHC-mismatched) RPE cells transplanted into the cynomolgus macaque eye.[22] In that study, it was concluded that allogeneic RPE cells were rejected by the immune system, as evidenced by subretinal fibrosis observed in color fundus photographs; however, the animals were maintained until 1 year posttransplantation, and no histological evidence was provided to validate this conclusion. A follow-up study by the same group did include a histological analysis at 8, 12, and 26 weeks posttransplantation that supported their previous conclusions that the allogeneic RPE cells were rejected.[23] Although these studies lend support to the hypothesis that allogeneic RPE cells transplanted into the non–immune-suppressed subretinal space will be rejected by the immune system, the response of the nonhuman primate (NHP) immune system to transplanted allogeneic RPE cells within the first 8 weeks posttransplantation remains unexplored. The present study closely correlated in vivo imaging with histological analysis to systematically evaluate the short-term immune system response following transplantation of iPS-derived allogeneic RPE cells into the subretinal space of nonimmunosuppressed rhesus macaques.

Methods

Generation of Macaque RPE

Rhesus macaque iPS cells were generated from primary fibroblast cultures transduced with retroviral vectors as previously described.[24] Established iPS colonies were maintained on inactivated mouse embryonic fibroblast (mEF) cells in Dulbecco's modified Eagle's medium/F12 (Invitrogen, Carlsbad, CA, USA) supplemented with 15% fetal bovine serum (HyClone, Erie, UK), 1% nonessential amino acids (Invitrogen), 2 mM L-glutamine (Invitrogen), 0.1 mM β-mercaptoethanol (Sigma-Aldrich, St. Louis, MO, USA), and 1% penicillin streptomycin (Invitrogen). On 80% confluence, iPS colonies were incubated with 1 mg/mL collagenase and gently collected using a cell lifter (Corning Inc., Corning, NY, USA). Intact colonies were plated on low-attachment six-well plates (Corning) for embryoid body formation followed by distribution on Matrigel (BD Biosciences, San Jose, CA, USA) -coated plates. RPE differentiation was directed by exposing cells to knockout serum replacement media supplemented with Noggin (R&D Systems, Minneapolis, MN, USA), SB431542 (Tocris, Bristol, UK), Activin A (R&D Systems), and nicotinamide (Sigma-Aldrich, St. Louis, MO, USA),[25] a protocol similar to previously published differentiation methods for human RPE.[26–30] Pigmented colonies were manually picked, dissociated with trypsin, and plated on Primaria plates (BD Biosciences) in THT medium for further enrichment.[31,32] RPE cells were transduced to express green fluorescent protein (GFP) using AAV2-CMV-eGFP a minimum of 2 weeks before transplantation. In vitro characterization of RPE cells included PCR and immunocytochemistry. Total RNA was extracted (RNeasy Kit; Qiagen, Valencia, CA, USA) from iPS cell–derived RPE, and PCR reactions were performed for RPE65, pigment-epithelium-derived factor (PEDF), cellular retinaldehyde-binding protein (CRALBP), Bestrophin-1 (BEST1), zonula occludens protein 1 (ZO-1), and microphthalmia-associated transcription factor (MITF). Additional cells were plated on Nunc Lab-Tek II chamber slides (Sigma-Aldrich) for immunostaining using antibodies against RPE65, 1:250 (Abcam, Cambridge, UK); ZO-1, 1:100 (Invitrogen); CRALBP, 1:100 (Abcam); premelanosome (PMEL) 17, 1:500 (Abcam); and MITF, 1:100 (Millipore, Billerica, MA, USA).

Animal Model and Surgical Method

Six adult female rhesus macaques (*Macaca mulatta*), ages 7 to 12 years, were used for this study. All experiments were approved by the Institutional Animal Care and Use Committee at Oregon Health & Science University, and adhered to the ARVO Statement for the Use of Animals in Ophthalmic and Vision Research. In previous studies, a transretinal surgical approach was used to deliver RPE cells to the subretinal space in NHPs; however, this approach has been shown to result in leakage of RPE cells into the vitreous cavity that would have complicated interpretation of the results of this study.[33] Instead, for this study, cells were delivered into all 12 eyes using a two-step technique as described in detail previously.[33] In summary, a subretinal saline bleb was created using a 41-gauge cannula (#5194; Microvision, Redmond, WA, USA) using a pars plana trans-vitreal approach, after which 500,000 GFP-labeled iPS-derived RPE cells in 50 μL were injected transsclerally into the preformed bleb using a 30-gauge angulated

Table. Survival Time After Cell Transplantation

Animal	Eye	Postsurgery Histology Time-Point
Subject 1	OS	7 wk
Subject 1	OD	3 wk
Subject 2	OS	7 wk
Subject 2	OD	3 wk
Subject 3	OS	7 wk
Subject 3	OD	3 wk
Subject 4	OS	7 wk
Subject 4	OD	3 wk
Subject 5	OS	4 d
Subject 5	OD	4 d
Subject 6	OS	1 d
Subject 6	OD	2 h

sharp tip cannula (#7509; Hurricane Medical, Bradenton, FL, USA). After the sclera and conjunctiva were sutured closed, dexamethasone (0.5 mL, 10 mg/mL) and cefazolin (0.5 mL, 125 mg/mL) were administered subconjunctivally, and dexamethasone (1%) and ofloxacin (0.3%) eye drops were applied twice daily for 1 week. Using this technique,[33] we transplanted allogeneic iPS-RPE cells into the subretinal space of one animal specifically for a short-term time point in which cells were injected into the first eye on day 0 and then on the following day (day 1) into the contralateral eye. The animal was euthanized 2 hours after the second injection, providing a 2-hour and approximately 24-hour postinjection time point for histological analysis. A second animal received transplantation of RPE cells in both eyes on day 0 and was euthanized 4 days later. The remaining four animals received transplantations of RPE cells into the first eye on day 0 followed by transplantation into the contralateral eye 4 weeks later, and all four were euthanized after an additional 3 weeks (see Table for a summary).

Retinal Imaging

Each animal received a comprehensive panel of retinal imaging before transplantation (baseline), at postoperative days 4 and 7, and weekly thereafter until animals were euthanized. For each imaging session, monkeys were anesthetized by an intramuscular injection of Telazol (1:1 mixture of tiletamine hydrochloride and zolazepam hydrochloride, 3.5–5.0 mg/kg) and maintained with ketamine (1–2 mg/kg) as required; or were sedated with ketamine (10 mg/kg intramuscularly [IM]) or Telazol (3–5 mg/kg IM) followed by intubation and anesthesia with inhalant isoflurane (1%–2%) vaporized in oxygen. Supplemental oxygen was provided as needed via nasal cannula at 0.5 to 1.0 L/min, and heart rate and peripheral blood oxygen saturation were monitored by pulse oximetry. Rectal temperature was maintained between 37.0°C and 38.0°C by water-circulating heated pads. For image acquisition, animals were positioned prone with the head supported by a chinrest; and the pupils were dilated to a minimum of 8 mm using phenylephrine (2.5%; Bausch and Lomb, Rochester, NY, USA) and tropicamide (1% Tropicacyl; Akorn, Lake Forest, IL, USA) eye drops. Eyelid specula were used to keep the eyelids open and clear plano contact lenses were inserted centered over the cornea. Imaging modalities included color fundus photography (FF450; Zeiss, Oberkochen, Germany), spectral domain optical coherence tomography and fundus autofluorescence (OCT/FAF; Heidelberg Spectralis, Heidelberg, Germany). Baseline OCT scans of both eyes were acquired over a 30 × 20-degree field with 61 b-scans centered on the macula, with each slice consisting of the average of approximately 20 images. In vivo retinal fundus autofluorescence elicited by short-wavelength (488 nm) excitation was obtained as described previously.[34] In addition, OCT and FAF scans were collected in temporal retina in the planned location of the subretinal bleb and deposition of transplanted cells. Posttransplantation imaging was performed as repeated (coregistered) scans if possible. Spectralis segmentation software (Heidelberg Eye Explorer 1.9.10.0) was used to segment the retinal layers, with subsequent inspection and manual correction by a second skilled observer. Following imaging, the contact lenses and eyelid specula were removed, and erythromycin ointment was applied to each eye. Animals were then recovered from sedation and returned to their home cages or enclosures.

Histology/Immunohistochemistry

After animals were euthanized, eyes were collected and immersion fixed in 4% paraformaldehyde in phosphate buffered saline for 24 to 48 hours. Whole eyes collected from monkeys with 2 days or less postinjection period were embedded in paraffin and sectioned at 5 μm, and selected sections were stained with hematoxylin-eosin (H&E). Eyes collected at longer postinjection survival times were hemisected and the anterior chamber and vitreous removed. The posterior half of the globe was then cryoprotected in increasing sucrose gradients (up to 30%), embedded in optimum cutting temperature compound, and frozen in an embedding mold. Frozen blocks were sectioned at 14 μm using a cryostat (CM1850; Leica, Wetzlar, Germany). Two sections per slide were collected in a five-slide series. The first slide of each series (slide 1, 6, 11, and so on), which provided a tissue section every 70 μm throughout the eye, was stained using cresyl violet acetate. Cresyl violet– and H&E-stained sections were examined for subretinal bleb injection site retinotomy, transscleral injection site, evidence of transplanted cells, evidence of immunological reaction, and any signs of pathology. Following examination of the stained sections, slides adjacent to those with notations of the five points listed above were used for immunohistochemical study. Transplanted cells were identified by colocalization of GFP fluorescence and staining with anti-RPE65 or anti-PMEL17 antibodies. Immune infiltrates were identified using antibodies against T cells (CD3), B cells (CD20), and microglial/macrophage cells (Iba1). All primary antibodies were used at a concentration of 1:500, and detection of primary antibodies was achieved using Alexafluor secondary antibodies at a concentration of 1:300; 4′,6-diamidino-2-phenylindole (DAPI) was used as a nuclear marker counterstain.

Results

Generation and Transplantation of NHP iPS-RPE

Generation of RPE cells was performed using multiple iPSC lines with similar efficiency to that reported previously in NHPs[22,35–40]; however, only one line was used for expansion and transplantation studies in this study. The RPE cells were heavily pigmented, mostly hexagonal in shape, and expressed markers consistent with primary RPE cells, including RPE65, CRABP, MITF, PEDF, BEST1, and ZO-1 by PCR and immunohistochemistry (Fig. 1). Transduction of GFP was successful in all RPE cells with no evidence of cell death or impairment. On each surgical day, cultured cells were trypsinized (0.25%), washed, centrifuged (3 minutes at 250*g*), and resuspended in sterile balanced salt solution plus (BSS+) at a concentration of 10,000 cells per μL. Pre- and postsurgical cell viability measurements were performed and remained above 95% in each case.

Investigative Ophthalmology & Visual Science

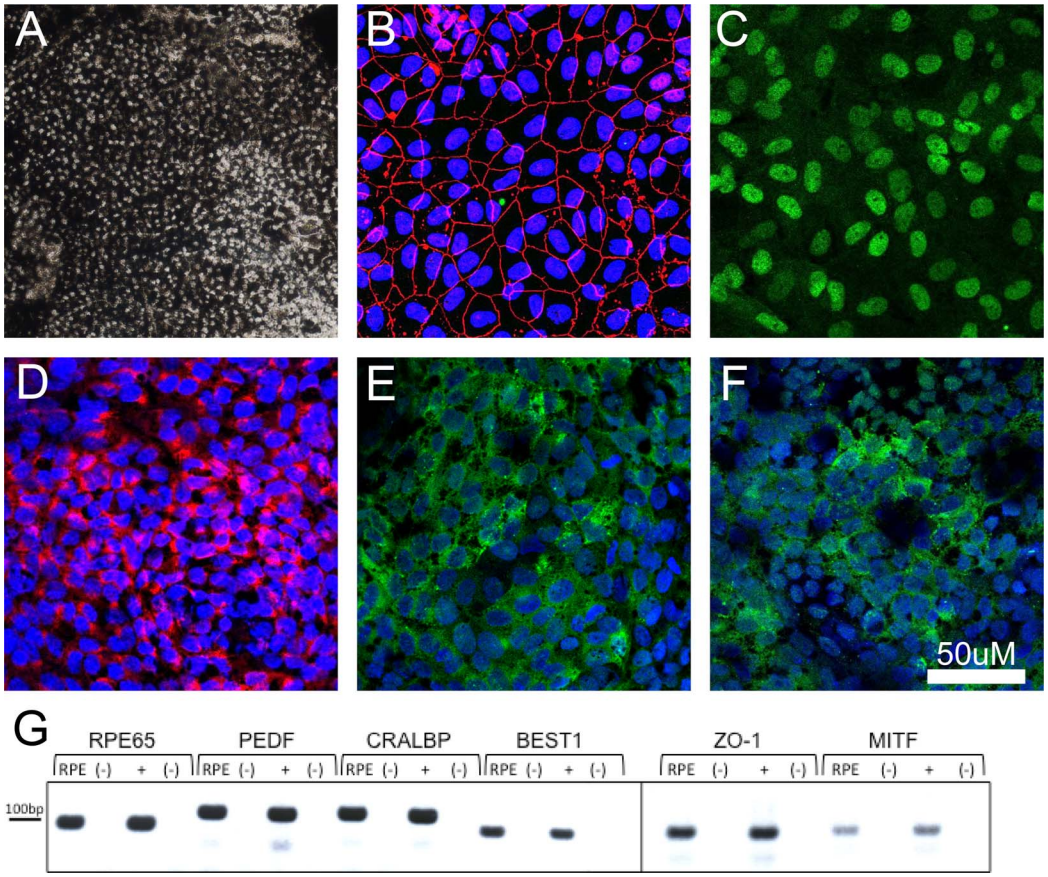

Figure 1. Characterization of rhesus monkey iPS-derived RPE cells. (**A**) Image captured from a confluent and mature plate of RPE cells. (**B–F**) Images of RPE cells stained with the immunohistochemical markers ZO-1 (**B**), MITF (**C**), PMEL17 (**D**), CRALBP (**E**), and RPE65 (**F**). (**G**) Expression of RPE-associated genes in iPS-derived RPE as demonstrated through RT-PCR. Headings for (**G**): RPE, Rhesus iPS-RPE cells; (+), rhesus primary RPE tissue; (-), no-RT controls for each reaction.

In Vivo Imaging of Transplanted Cells and Immune Rejection

In each eye, color fundus photographic images revealed a single subretinal detachment within the retinal arcades temporal to the fovea and extending peripherally. The edge of the bleb near the macula was clearly visible in all cell-injected eyes. In most instances, much of the detachment was visible even though the bleb often extended outside the photographed area. Delivery of cells into the subretinal space was successful in all 12 eyes, as indicated by visualization of GFP fluorescence in the subretinal space and a lack of GFP in the vitreous. In some cases, OCT/FAF imaging was performed immediately postinjection to confirm placement of cells (data not shown). Fluorescence of the transplanted cells was visualized in the subretinal space in five of six eyes imaged at 4 days posttransplantation and seven of eight eyes at 1 week, but the quantity of fluorescent cells clearly diminished over this period. Fluorescence of GFP-labeled cells was absent by 3 weeks posttransplantation in all cases. Patchy hyperpigmentation of the fundus was always observed in areas where transplanted cells were once located but fluorescence had since faded (Fig. 2, middle column) and occurred occasionally in other locations within the preformed bleb.

Baseline OCT imaging of all animals revealed normal retina and RPE structure. In all cases, the sterile BSS+ used to create the subretinal bleb was absorbed and the neural retina returned to apposition of the RPE by 1-week posttransplantation. At this time point, the transplanted cells were visualized primarily as large clusters of cells that were typically located near the edge of the preformed bleb. Additional small groups of cells were somewhat evenly distributed throughout the detachment (Fig. 2, right column). With decreasing numbers of transplanted cells in each clump came increasing difficulty in their visualization using OCT, although the cells could still be identified using GFP fluorescence. Despite the progressive loss of GFP fluorescence of the transplanted cells, optically reflective cellular material could be identified in the subretinal space by OCT at all time points up to 7 weeks posttransplantation (Fig. 2, right column).

Initial indications of immune reaction in vivo were observed as early as 4 days postinjection; in particular, subretinal fibrosis observed as white or pale fibrosis in color fundus images was observed in 75% of eyes at 4 days postinjection and remained until animals were euthanized (Fig. 2, left column). However, there was no evidence of disc redness, persistent serous detachments, or edema. No vitreous or anterior chamber inflammatory cells were observed. Opacity of the vitreous was seen in only one case, resolved within a week, and was attributed to intra- or postoperative hemorrhage. Except at the site of retinotomy used to create the subretinal bleb, the neural retina did not appear to suffer significant damage anywhere else in the eye.

Histological Analysis of Inflammatory Response

Imaging of GFP epifluorescence in frozen sections stained with cresyl violet acetate indicated that the GFP-positive transplant-

Investigative Ophthalmology & Visual Science

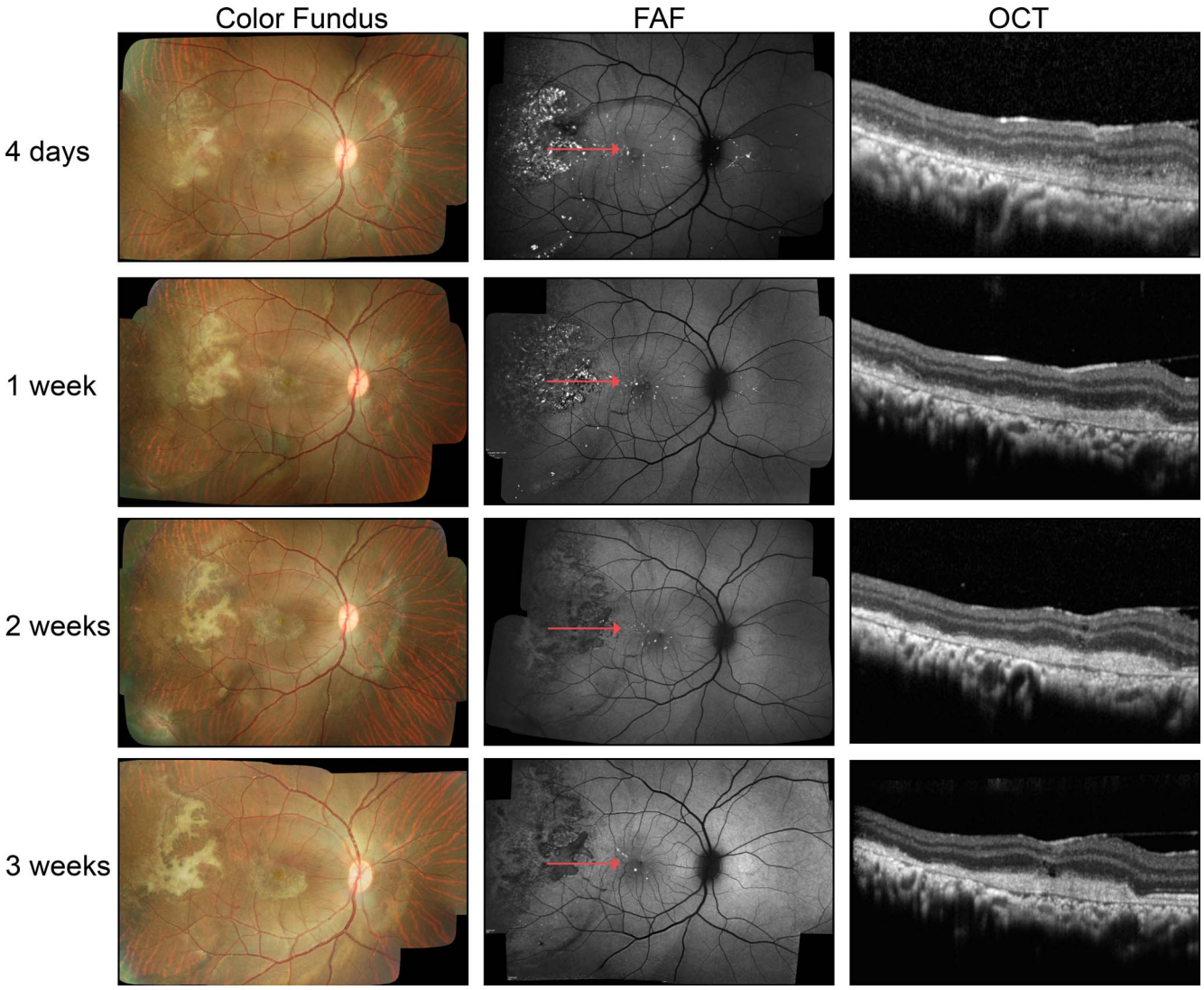

Figure 2. In vivo imaging of GFP-labeled RPE cells transplanted into the subretinal space of non–immune-suppressed rhesus monkeys using color fundus photography, FAF, and OCT at 4 days and 1, 2, and 3 weeks posttransplantation. In the representative color fundus images, white subretinal material was present at 4 days and evolved in shape and appearance over subsequent weeks. The GFP fluorescence of the transplanted cells was evident at 4 days but extinguished by 2 weeks. Subretinal debris, fibrotic scarring, and mononuclear cells, as confirmed by histology, resulted in OCT images that showed material in the subretinal space that without confirmation through histologic study could be misinterpreted as the transplanted RPE cells.

ed cells were located in the subretinal space at 1 and 4 days but were no longer present at 3 weeks posttransplantation (Figs. 3, 4). At localized areas within the transplantation zone, a prominent mononuclear cell infiltrate was evident throughout the choroid and in the subretinal space as early as 4 days and persisted through 3 weeks posttransplantation (Fig. 4). At 7 weeks posttransplantation, nearly all the inflammatory cell infiltrate had resolved, with only a few highly pigmented cells remaining within a fibrotic scar. Immunohistochemical analysis revealed a differential time course for infiltration by inflammatory cell types. No inflammatory cells were evident at 2- or 24-hour time points (not shown). T cells (CD3 positive) were most prevalent at 4 days but reduced in number by 3 weeks; whereas a few B cells (CD20 positive) appeared at 4 days, but increased in number at 3 weeks. All T and B cells were absent at 7 weeks posttransplantation. Microglial cells (Iba1 positive) were present throughout the choroid and subretinal space in the area of the bleb at 4 days through 3 weeks, but had resolved by 7 weeks (Fig. 4). Trem2 and Tmem119 antibodies were used to further characterize microglial and macrophage cells; however, immunoreactivity in NHP tissue was poor, the staining was inconclusive despite multiple repeats, and thus these data are not presented. The inflammatory response was precisely localized to areas of retina containing transplanted cells and there was minimal disruption to the apposed neural retina, and seemingly no disruption to RPE and photoreceptor layers outside the area of the bleb (Fig. 5). However, at locations within the bleb where mononuclear infiltrates or subretinal scarring were present, areas of host RPE were absent (Fig. 6). The areas of host RPE loss corresponded to areas of hypo-autofluorescence observed in FAF imaging.

Discussion

This study demonstrates failure of allogeneic iPS-derived RPE cell transplants into the subretinal space of nonimmunosuppressed NHPs, likely due to rejection by the immune system. A

Investigative Ophthalmology & Visual Science

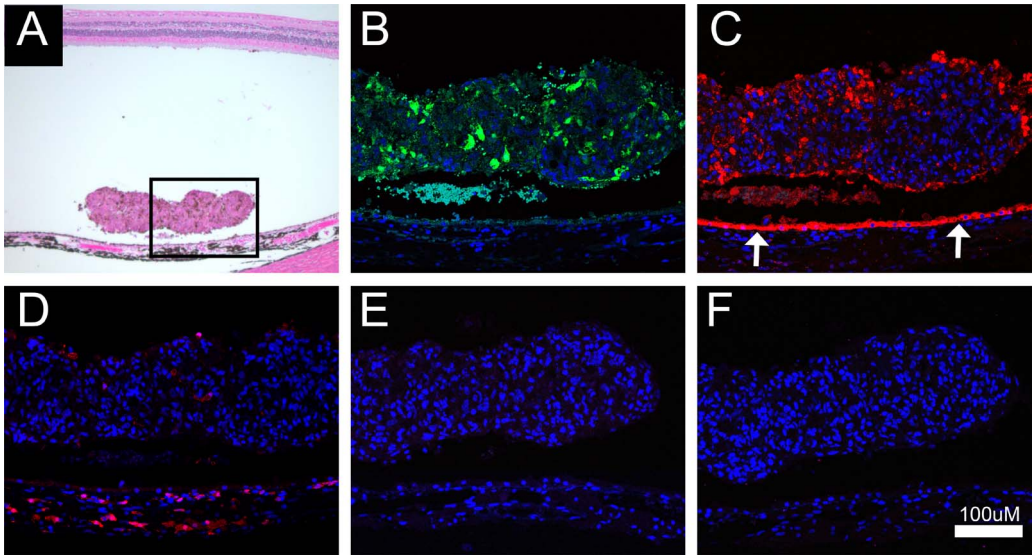

FIGURE 3. Histological analysis of RPE cell transplantation 1 day postinjection. (**A**) A clump of transplanted cells in the subretinal space; the retina had not yet reattached to the RPE. (**B**) GFP epifluorescence of the transplanted cells (*green*). (**C**–**F**) Immunohistochemical identification of the transplanted cells and host RPE (*arrows*) using RPE65 (**C**; *red*), microglial cells in the choroid and a few comingled with the transplanted cells (**D**; *red*), and the absense of T (**E**; CD3) or B cells (**F**; CD20) at this time point.

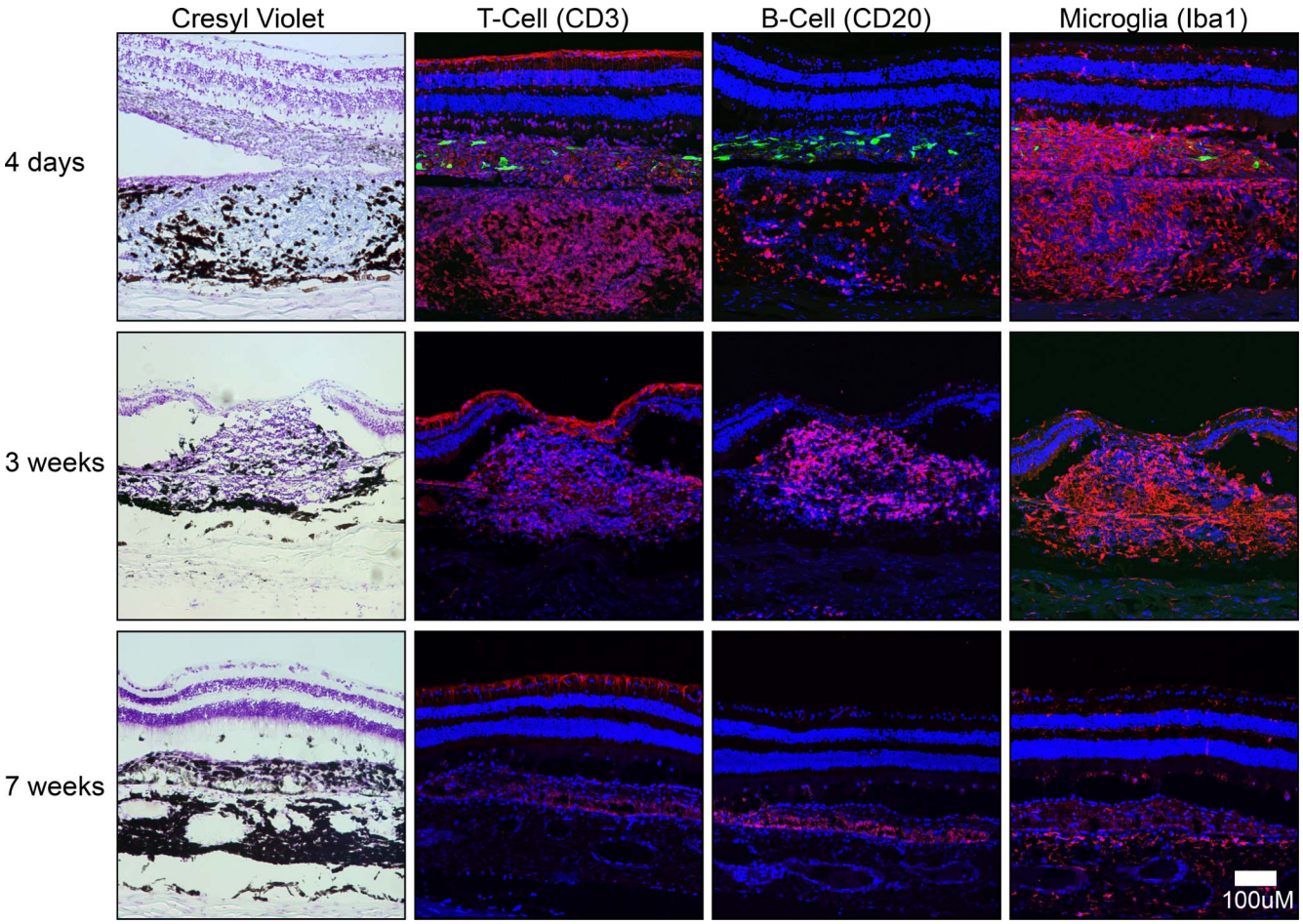

FIGURE 4. Histological and immunohistochemical analysis in non–immune-suppressed rhesus monkeys at 4 days, 3 weeks, and 7 weeks following transplantation. Cresyl violet staining was used to determine the locations of mononuclear cell infiltration; Anti-CD3 antibody was used to detect T cells, anti-CD20 to detect B cells, and anti-Iba1 to detect macrophages and retinal microglia (all *red*). Transplanted RPE cells were evident in tissue sections at 4 days (GFP, *green*). A strong T-cell and microglial response was evident at 4 days. At 3 weeks, the T-cell response was reduced, but the microglial cell response remained and B-cell response increased. By 7 weeks, T-cell, B-cell, and microglial/macrophage responses had all resolved.

Investigative Ophthalmology & Visual Science

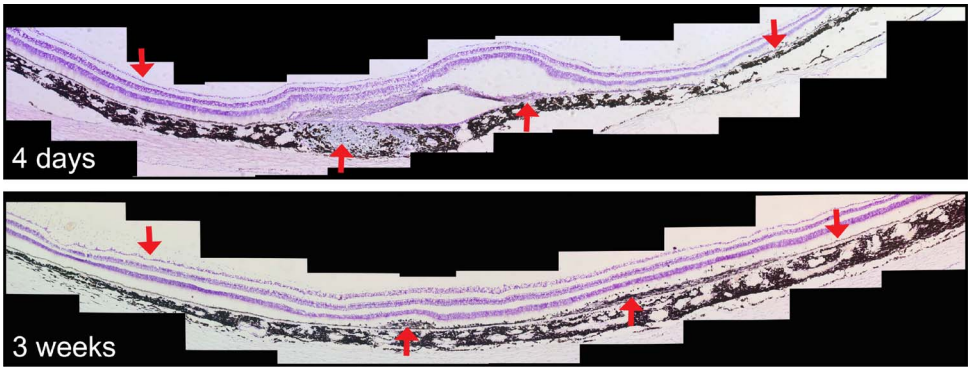

Figure 5. Image montage of cresyl violet–stained retina sectioned horizontally through the location of the RPE cell transplant. *Upward red arrows* indicate the location of mononuclear cell infiltration and fibrotic scarring; *downward arrows* indicate loci of normal RPE and neural retina outside the transplant area.

strong inflammatory response occurred in a highly localized and aggressive manner by 4 days posttransplantation, continued through 3 weeks, and resolved by 7 weeks posttransplantation. Death of the transplanted RPE cells was evident by in vivo imaging as the loss of GFP fluorescence measured by FAF, and the simultaneous formation, in most cases, of a well-demarcated subretinal plaque seen in color photographs. Notably, there were no overt clinical signs of inflammation, such as vitreous cells, retinal edema, or persistent subretinal fluid. Immunohistochemical analysis at multiple time points illustrated the progression from primarily a microglial and T-cell–mediated response at 4 days to a microglial and B-cell response at 3 weeks, with resolution of the response by 7 weeks following transplantation. Localized choroidal thickening with a dense infiltrate of mononuclear cells and microglia was evident in all cases. The inflammatory response was restricted to the locations of the transplanted cells. The mononuclear response was not evident outside the area of retina that had been surgically detached. In addition, systemic/peripheral lymphocyte activation was below detectable levels (measured weekly in blood, data not shown), emphasizing the highly localized nature of the intraocular response.

The observed inflammatory response in our study appeared to be mediated initially by microglia/macrophages and T cells, thus showing key features of the classic immunologic rejection response to foreign grafts.[41–43] This finding is also consistent with a recent study that evaluated the survival of allogeneic iPSC-derived RPE cells following transplantation into the subretinal space of pigs.[21] In that study, the iPS-RPE cells survived in the subretinal space for approximately 3 weeks posttransplantation, at which time T-cell and macrophage activation were observed in the choroid and subretinal space. Although other studies also have observed an immune response following transplantation of iPS-derived RPE into NHPs,[22,44] our study is the first to characterize the nature and time course of inflammatory reaction following transplantation of allogeneic cells in the primate eye. Collectively, these studies suggest that the subretinal space in normal NHPs may lose its immune privilege properties in cases of surgical manipulation of the retina or RPE. Thus, it is likely the same would hold true for normal human eyes and eyes with diseases such as AMD.

We cannot exclude the possibility that materials common to iPS cell generation or cell culture in general (e.g., vectors, fetal bovine serum, laminins) may provide antigens contributing to the immunologic reaction in this study. This possibility seems less likely given the many times the cells were washed before transplantation, the very low concentration of these materials, the long duration of cells in culture after exposure to some of these elements (up to 6 months in cases such as RPE cells), and evidence from previous studies indicating that transplantation of other cell types, such as neural progenitor cells, that use these common materials do not invoke such an inflammatory response.[45]

In this study, we were able to acquire a series of high-quality retinal images using color fundus photography, fundus autofluorescence, and OCT, and then confirm and correlate our findings by histological and immunohistochemical evaluation. Our results suggest that a number of changes in ocular structure, such as thickening of the choroid combined with or as a result of infiltration of mononuclear cells, can be subtle and go unnoticed using today's imaging technologies. In addition, OCT imaging of the subretinal space provided misleading information, as the transplanted RPE cells that provided significant GFP fluorescence and OCT reflectance

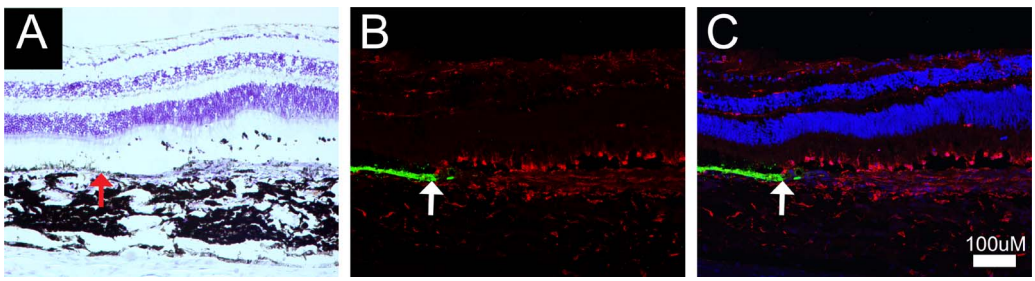

Figure 6. Representative example of the loss of host RPE in the area corresponding to mononuclear cell infiltration, microglial cell presence, and fibrotic scarring. (**A**) Image of a cresyl violet–stained section at the border of host RPE loss highlighted by the *upward red arrow*. (**B**) Immunofluorescent image of RPE65 (*green*) and microglial cells (*red*) at the border of host RPE loss (*white arrow*). (**C**) Same as (**B**) plus DAPI.

Investigative Ophthalmology & Visual Science

shortly after transplantation were quickly replaced with inflammatory cells. Although GFP fluorescence disappeared, OCT reflectance persisted, making it impossible to discriminate between transplanted RPE cells and the infiltrating immune reaction. Although all early-phase clinical trials to date have established a safety profile for transplantation of allogeneic RPE cells into AMD patients and others with retinal disease, one cannot discount the possibility that in each of these studies, RPE transplants were rejected shortly following implantation, but this process was not detected. Finally, hypofluorescence observed in FAF imaging in this study corresponded to the same locations at which host RPE cells were lost, presumably to a bystander immune response. In addition, in areas of inflammatory cell infiltration, there was an accumulation of pigmented debris in all cases. Thus, increases in pigmentation do not necessarily reflect a surviving RPE cell transplant. Hypopigmentation may reflect loss of host RPE, which would present a cause for concern when treating RPE-related disorders. These correlates of histology and clinical imaging can be of great assistance in interpreting the imaging findings in human trials of RPE transplants.

It is important to consider alternative explanations for the lack of survival of the transplanted cells in this study. For instance, the observed immune reaction could have been secondary to death of the transplanted cells from the transplant procedure, rather than the cause of the cell death. This seems unlikely given the favorable survival rates of the control aliquots of cells, and the fact that a similar injection procedure in rodents has resulted in long-term survival of RPE cells.[7–10] Another possibility is that GFP, which is known to have potential cytotoxic properties, is responsible for initiation of the immune response and ultimately responsible for graft failure. We think this is unlikely, because our previous cell transplantation of GFP-labeled neural progenitor cells into the NHP eye did not result in graft rejection.[45] In addition, although GFP immunogenicity is postulated to be T-cell mediated, many preclinical studies of retinal gene therapy have used GFP as a reporter protein without similar immune-related issues.[46]

Another consideration is the generalizability of our results, that is, whether other types of cells might face different outcomes from the iPS cell–derived RPE cell line used in this study. Although lymphocyte activation was not observed in our previous study using human neural progenitor cells (either with or without immune suppression),[45] the answer to that question cannot be known without testing other cell lines and evaluating the immune response under similar circumstances. A number of other non–iPS cell–derived sources of cells are being developed for the treatment of retinal degenerative disease, including those from mesenchymal cells and bone marrow, and testing of each cell source for safety and efficacy would be highly informative.[5,17,47–50]

The purpose of this study was to characterize the consequences of allogeneic RPE cell transplantation into the NHP eye under non–immune-suppressed conditions. Some have suggested that the relative immune privilege of the subretinal space alone could permit cell survival. Although immune suppressants are well tolerated by monkeys, it was important to document whether and how the immune system would react in response to the engrafted cells without immune suppression to serve as baseline data for future studies that do use immune suppression and those that use cells from autologous sources. In addition, the demonstration that microglial cells play a critical role in this rejection process emphasizes the need for future evaluations of cell survival following microglial cell inhibition as an alternative immune-suppression approach. The data generated here also provide the baseline for evaluations of which immune-suppressive drugs and at what dosages might best protect the grafts to prevent rejection.

In summary, we have demonstrated a timeline of the natural immunological response to transplanted allogeneic RPE cell in the non–immune-suppressed NHP eye. Our data demonstrate a rapid failure of the graft. Ultimately, success of RPE transplantation for the treatment of AMD and other RPE disorders will involve balancing the risks of surgery with the beneficial effects of the cell transplantation, which rely heavily on the survival of the transplanted cells. The present study highlights the importance of immune-related issues in cell transplantation to treat retinal disease and underscores the need for substantial further understanding of transplant immunology in the eye.

Acknowledgments

The authors thank Steven Bailey and Tim Stout for their surgical expertise, and Emily Johnson, Robert Bonnah, Kasie Paul, Rebecca Tipner-Hodges, Hong Ma, and the staff of the Department of Comparative Medicine at the Oregon National Primate Research Center (ONPRC) for their valuable technical assistance and support.

Supported by grant R01EY021214 (MN) and core grants P30 EY010572 (Casey Eye Institute) and P51OD011092 (ONPRC) from the National Institutes of Health (Bethesda, MD, USA), an unrestricted grant to the Casey Eye Institute from Research to Prevent Blindness, the Wold Macular Degeneration Lab, the Campbell Stem Cell Lab, the Sybil B. Harrington Special Scholar Award from Research to Prevent Blindness (TJM), and grants from the Foundation Fighting Blindness (MN).

Disclosure: **T.J. McGill**, None; **J. Stoddard**, None; **L.M. Renner**, None; **I. Messaoudi**, None; **K. Bharti**, None; **S. Mitalipov**, None; **A. Lauer**, None; **D.J. Wilson**, None; **M. Neuringer**, None

References

1. Friedman DS, O'Colmain BJ, Munoz B, et al. Prevalence of age-related macular degeneration in the United States. *Arch Ophthalmol*. 2004;122:564–572.
2. Bird AEC, Bressler NM, Bressler SB, et al. An international classification and grading system for age- related maculopathy and age-related macular degeneration. *Surv Ophthalmol*. 1995;39:367–374.
3. Klein R, Peto T, Bird A, Vannewkirk MR. The epidemiology of age-related macular degeneration. *Am J Ophthalmol*. 2004; 137:486–495.
4. Haddad S, Chen CA, Santangelo SL, Seddon JM. The genetics of age-related macular degeneration: a review of progress to date. *Surv Ophthalmol*. 2006;51:316–363.
5. Sun J, Mandai M, Kamao H, et al. Protective effects of human iPS-derived retinal pigmented epithelial cells in comparison with human mesenchymal stromal cells and human neural stem cells on the degenerating retina in rd1 mice. *Stem Cells*. 2015;33:1543–1553.
6. Li Y, Tsai YT, Hsu CW, et al. Long-term safety and efficacy of human-induced pluripotent stem cell (iPS) grafts in a preclinical model of retinitis pigmentosa. *Mol Med*. 2012;18: 1312–1319.
7. Lu B, Malcuit C, Wang S, et al. Long-term safety and function of RPE from human embryonic stem cells in preclinical models of macular degeneration. *Stem Cells*. 2009;27:2126–2135.
8. Carr AJ, Vugler AA, Hikita ST, et al. Protective effects of human iPS-derived retinal pigment epithelium cell transplantation in the retinal dystrophic rat. *PLoS One*. 2009;4:e8152.
9. Wang S, Lu B, Girman S, Holmes T, Bischoff N, Lund RD. Morphological and functional rescue in RCS rats after RPE cell

line transplantation at a later stage of degeneration. *Invest Ophthalmol Vis Sci*. 2008;49:416–421.

10. Lund RD, Wang S, Klimanskaya I, et al. Human embryonic stem cell-derived cells rescue visual function in dystrophic RCS rats. *Cloning Stem Cells*. 2007;8:189–199.
11. Wang S, Lu B, Wood P, Lund RD. Grafting of ARPE-19 and Schwann cells to the subretinal space in RCS rats. *Invest Ophthalmol Vis Sci*. 2005;46:2552–2560.
12. McGill TJ, Lund RD, Douglas RM, Wang S, Lu B, Prusky GT. Preservation of vision following cell-based therapies in a model of retinal degenerative disease. *Vision Res*. 2004;44:2559–2566.
13. Schwartz SD, Hubschman JP, Heilwell G, et al. Embryonic stem cell trials for macular degeneration: a preliminary report. *Lancet*. 2012;379:713–720.
14. Schwartz SD, Tan G, Hosseini H, Nagiel A. Subretinal transplantation of embryonic stem cell-derived retinal pigment epithelium for the treatment of macular degeneration: an assessment at 4 years. *Invest Ophthalmol Vis Sci*. 2016;57:ORSFc1–ORSFc9.
15. Cuenca N, Fernandez-Sanchez L, McGill TJ, et al. Phagocytosis of photoreceptor outer segments by transplanted human neural stem cells as a neuroprotective mechanism in retinal degeneration. *Invest Ophthalmol Vis Sci*. 2013;54:6745–6756.
16. McGill TJ, Cottam B, Lu B, et al. Transplantation of human central nervous system stem cells - neuroprotection in retinal degeneration. *Eur J Neurosci*. 2012;35:468–477.
17. Lu B, Wang S, Girman S, McGill T, Ragaglia V, Lund R. Human adult bone marrow-derived somatic cells rescue vision in a rodent model of retinal degeneration. *Exp Eye Res*. 2010;91:449–455.
18. Lu B, Wang S, Francis PJ, et al. Cell transplantation to arrest early changes in an ush2a animal model. *Invest Ophthalmol Vis Sci*. 2010;51:2269–2276.
19. Wang S, Girman S, Lu B, et al. Long-term vision rescue by human neural progenitors in a rat model of photoreceptor degeneration. *Invest Ophthalmol Vis Sci*. 2008;49:3201–3206.
20. McGill TJ, Lund RD, Douglas RM, et al. Syngeneic Schwann cell transplantation preserves vision in RCS rat without immunosuppression. *Invest Ophthalmol Vis Sci*. 2007;48:1906–1912.
21. Sohn EH, Jiao C, Kaalberg E, et al. Allogenic iPSC-derived RPE cell transplants induce immune response in pigs: a pilot study. *Sci Rep*. 2015;5:11791.
22. Kamao H, Mandai M, Okamoto S, et al. Characterization of human induced pluripotent stem cell-derived retinal pigment epithelium cell sheets aiming for clinical application. *Stem Cell Reports*. 2014;2:205–218.
23. Sugita S, Iwasaki Y, Makabe K, et al. Lack of T cell response to iPSC-derived retinal pigment epithelial cells from HLA homozygous donors. *Stem Cell Reports*. 2016;7:619–634.
24. Tachibana M, Ma H, Sparman ML, et al. X-chromosome inactivation in monkey embryos and pluripotent stem cells. *Dev Biol*. 2012;371:146–155.
25. Ferrer M, Corneo B, Davis J, et al. A multiplex high-throughput gene expression assay to simultaneously detect disease and functional markers in induced pluripotent stem cell-derived retinal pigment epithelium. *Stem Cells Transl Med*. 2014;3:911–922.
26. McGill TJ, Bohana-Kashtan O, Stoddard JW, et al. Long-term efficacy of GMP grade xeno-free hESC-derived RPE cells following transplantation. *Trans Vis Sci Tech*. 2017;6(3):17.
27. Idelson M, Alper R, Obolensky A, et al. Directed differentiation of human embryonic stem cells into functional retinal pigment epithelium cells. *Cell Stem Cell*. 2009;5:396–408.
28. Tannenbaum SE, Turetsky TT, Singer O, et al. Derivation of xeno-free and GMP-grade human embryonic stem cells—platforms for future clinical applications. *PLoS One*. 2012;7:e35325.
29. Buchholz DE, Pennington BO, Croze RH, Hinman CR, Coffey PJ, Clegg DO. Rapid and efficient directed differentiation of human pluripotent stem cells into retinal pigmented epithelium. *Stem Cells Transl Med*. 2013;2:384–393.
30. Maruotti J, Wahlin K, Gorrell D, Bhutto I, Lutty G, Zack DJ. A simple and scalable process for the differentiation of retinal pigment epithelium from human pluripotent stem cells. *Stem Cells Transl Med*. 2013;2:341–354.
31. Miyagishima KJ, Wan Q, Corneo B, et al. In pursuit of authenticity: induced pluripotent stem cell-derived retinal pigment epithelium for clinical applications. *Stem Cells Transl Med*. 2016;5:1562–1574.
32. Maminishkis A, Chen S, Jalickee S, et al. Confluent monolayers of cultured human fetal retinal pigment epithelium exhibit morphology and physiology of native tissue. *Invest Ophthalmol Vis Sci*. 2006;47:3612–3624.
33. Wilson DJ, Neuringer M, Stoddard J, et al. Subretinal cell-based therapy: an analysis of surgical variables to increase cell survival. *Retina*. 2017;37:2162–2166.
34. McGill TJ, Renner LM, Neuringer M. Elevated fundus autofluorescence in monkeys deficient in lutein, zeaxanthin, and omega-3 fatty acids. *Invest Ophthalmol Vis Sci*. 2016;57:1361–1369.
35. Torrez LB, Perez Y, Yang J, Zur Nieden NI, Klassen H, Liew CG. Derivation of neural progenitors and retinal pigment epithelium from common marmoset and human pluripotent stem cells. *Stem Cells Int*. 2012;2012:417865.
36. Shirai H, Mandai M, Matsushita K, et al. Transplantation of human embryonic stem cell-derived retinal tissue in two primate models of retinal degeneration. *Proc Natl Acad Sci U S A*. 2016;113:E81–E90.
37. Osakada F, Ikeda H, Sasai Y, Takahashi M. Stepwise differentiation of pluripotent stem cells into retinal cells. *Nat Protoc*. 2009;4:811–824.
38. Takahashi M, Haruta M. Derivation and characterization of lentoid bodies and retinal pigment epithelial cells from monkey embryonic stem cells in vitro. *Methods Mol Biol*. 2006;330:417–429.
39. Haruta M, Sasai Y, Kawasaki H, et al. In vitro and in vivo characterization of pigment epithelial cells differentiated from primate embryonic stem cells. *Invest Ophthalmol Vis Sci*. 2004;45:1020–1025.
40. Okamoto S, Takahashi M. Induction of retinal pigment epithelial cells from monkey iPS cells. *Invest Ophthalmol Vis Sci*. 2011;52:8785–8790.
41. Nasr M, Sigdel T, Sarwal M. Advances in diagnostics for transplant rejection. *Expert Rev Mol Diagn*. 2016;16:1121–1132.
42. Ingulli E. Mechanism of cellular rejection in transplantation. *Pediatr Nephrol*. 2010;25:61–74.
43. Issa F, Schiopu A, Wood KJ. Role of T cells in graft rejection and transplantation tolerance. *Expert Rev Clin Immunol*. 2010;6:155–169.
44. Sugita S, Kamao H, Iwasaki Y, et al. Inhibition of T-cell activation by retinal pigment epithelial cells derived from induced pluripotent stem cells. *Invest Ophthalmol Vis Sci*. 2015;56:1051–1062.
45. Francis PJ, Wang S, Zhang Y, et al. Subretinal transplantation of forebrain progenitor cells in nonhuman primates: survival and intact retinal function. *Invest Ophthalmol Vis Sci*. 2009;50:3425–3431.
46. Bennett J, Maguire AM, Cideciyan AV, et al. Stable transgene expression in rod photoreceptors after recombinant adeno-

Investigative Ophthalmology & Visual Science

associated virus-mediated gene transfer to monkey retina. *Proc Natl Acad Sci U S A*. 1999;96:9920–9925.

47. Labrador-Velandia S, Alonso-Alonso ML, Alvarez-Sanchez S, et al. Mesenchymal stem cell therapy in retinal and optic nerve diseases: an update of clinical trials. *World J Stem Cells*. 2016; 8:376–383.
48. Rodriguez-Crespo D, Di Lauro S, Singh AK, et al. Triple-layered mixed co-culture model of RPE cells with neuroretina for evaluating the neuroprotective effects of adipose-MSCs. *Cell Tissue Res*. 2014;358:705–716.
49. Saraf SS, Cunningham MA, Kuriyan AE, et al. Bilateral retinal detachments after intravitreal injection of adipose-derived 'stem cells' in a patient with exudative macular degeneration. *Ophthalmic Surg Lasers Imaging Retina*. 2017;48:772–775.
50. Kuriyan AE, Albini TA, Townsend JH, et al. Vision loss after intravitreal injection of autologous "stem cells" for AMD. *N Engl J Med*. 2017;376:1047–1053.

Investigative Ophthalmology & Visual Science